Genes, Brain and Behavior
Official publication of the International Behavioural and Neural Genetics Society

Genes, Brain and Behavior (2014) **13:** 144–151 doi: 10.1111/gbb.12096

# Variants in the 1q21 risk region are associated with a visual endophenotype of autism and schizophrenia

**P. T. Goodbourn[†,‡,*], J. M. Bosten[†], G. Bargary[†,§], R. E. Hogg[†,¶], A. J. Lawrance-Owen[†] and J. D. Mollon[†]**

*[†]Department of Experimental Psychology, University of Cambridge, Cambridge, UK, [‡]School of Psychology, University of Sydney, Sydney, Australia, [§]Division of Optometry and Visual Science, City University London, London, and [¶]Centre for Vision and Vascular Science, Queen's University Belfast, Belfast, UK*
**Corresponding author: Dr P. T. Goodbourn, School of Psychology, Brennan MacCallum Building, University of Sydney, NSW 2006, Australia. E-mail: patrick.goodbourn@sydney.edu.au*

*Received 6 August 2013, revised 10 October 2013, accepted for publication 17 October 2013*

**Deficits in sensitivity to visual stimuli of low spatial frequency and high temporal frequency (so-called *frequency-doubled gratings*) have been demonstrated both in schizophrenia and in autism spectrum disorder (ASD). Such basic perceptual functions are ideal candidates for molecular genetic study, because the underlying neural mechanisms are well characterized; but they have sometimes been overlooked in favor of cognitive and neurophysiological endophenotypes, for which neural substrates are often unknown. Here, we report a genome-wide association study of a basic visual endophenotype associated with psychological disorder. Sensitivity to frequency-doubled gratings was measured in 1060 healthy young adults, and analyzed for association with genotype using linear regression at 642 758 single nucleotide polymorphism (SNP) markers. A significant association ($P = 7.9 \times 10^{-9}$) was found with the SNP marker rs1797052, situated in the 5′-untranslated region of *PDZK1*; each additional copy of the minor allele was associated with an increase in sensitivity equivalent to more than half a standard deviation. A permutation procedure, which accounts for multiple testing, showed that the association was significant at the $\alpha = 0.005$ level. The region on chromosome 1q21.1 surrounding *PDZK1* is an established susceptibility locus both for schizophrenia and for ASD, mirroring the common association of the visual endophenotype with the two disorders. PDZK1 interacts with *N*-methyl-D-aspartate receptors and neuroligins, which have been implicated in the etiologies of schizophrenia and ASD. These findings suggest that perceptual abnormalities observed in two different disorders may be linked by common genetic elements.**

Keywords: Autism, endophenotype, frequency doubling, genome-wide association study, schizophrenia, visual sensitivity

Molecular genetic methods have promised to accelerate our understanding of disorders such as schizophrenia and autism spectrum disorder (ASD). Yet the link between genotype and phenotype in these cases is not straightforward. Psychological disorders arise through complex interactions between genes, regulatory networks and environmental factors, and phenotypes can be difficult to define because diverse symptomatologies are grouped within a single diagnostic category. An attractive alternative is to investigate associations between genotypes and quantitative *endophenotypes* – functional abnormalities associated with a disorder, but which are likely to stand in a more immediate relationship with underlying genetic mechanisms (Gottesman & Gould 2003). The approach also allows the use of psychologically normal participants; this may be preferable to the use of patients, whose multiple deficits might interfere with the measurement of distinct phenotypes (Braff & Freedman 2002).

Proposed endophenotypes of psychological disorders include cognitive, neurophysiological and psychomotor measures, and these have previously been investigated with molecular genetic methods (Greenwood *et al.* 2011, 2012, 2013). Some disorders are also associated with anomalies of basic visual perception (Butler *et al.* 2008; Dakin & Frith 2005; Grinter *et al.* 2010; Simmons *et al.* 2009). Visual markers of psychological disorder are ideal candidates for genetic studies because their underlying neural mechanisms are relatively well characterized. However, no genome-wide association study to date has investigated their possible genetic basis.

Schizophrenic patients and children with ASD show deficits in processing stimuli of low spatial frequency and high temporal frequency – stimuli that vary gradually across space and are briefly flashed or rapidly flickered. Sensitivity to such stimuli is often taken to reflect the integrity of the magnocellular visual pathway. One example is the *frequency-doubled grating* – so called because of the apparent doubling in spatial frequency of the percept – which is thought to be well matched to the response properties of the smooth monostratified class of retinal ganglion cells (Maddess 2011). The usual stimulus comprises a sinusoidal luminance grating of low spatial frequency reversing in contrast at a high temporal frequency (Fig. 1a), although spatial frequency doubling is observed in many briefly flashed or rapidly drifting stimuli (Rosli *et al.* 2009). Schizophrenic patients show selective deficits in detecting misalignment between

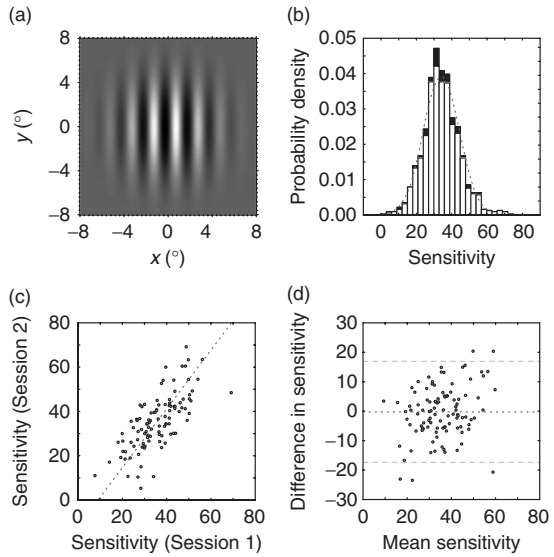


**Figure 1: Visual stimulus and psychophysical results**. (a) Normalized spatial luminance profile of the stimulus used in the study. (b) Distribution histogram of visual sensitivity. Light bars represent the genetic cohort ($N = 985$); light and dark bars combined represent the full psychophysical cohort ($N = 1057$). Probability density is relative to the psychophysical cohort. (c) Scatter plot of first- vs. second-session visual sensitivity for the retest subsample ($N = 104$). The dashed line shows the orthogonal linear regression to the data. (d) Bland–Altman plot of difference in sensitivity between sessions as a function of mean sensitivity across sessions ($N = 104$). The central dashed line shows the mean difference in sensitivity; upper and lower dashed lines show the limits of agreement (±1.96 SD of the difference).

low-contrast frequency-doubled gratings (Kéri *et al.* 2004, 2005a,b), and exhibit elevated thresholds for detecting gratings of low spatial frequency and high temporal frequency (Butler *et al.* 2005; Gracitelli *et al.* 2013). Autism spectrum disorder has also been associated with abnormal processing of these stimuli (Greenaway *et al.* 2013; McCleery *et al.* 2007): Greenaway *et al.*, for example, found that children with ASD were strikingly and selectively impaired in sensitivity to a large, briefly flashed target. In their sample, more than 40% of the children with ASD exhibited significantly elevated thresholds on an individual basis.

Here, we have measured sensitivity to frequency-doubled gratings in a large sample of healthy young adults. We report a genome-wide association analysis showing that individual differences in sensitivity are associated with the gene *PDZK1*, which lies in the 1q21.1 risk region for schizophrenia and ASD.

## Materials and methods

### Participants

Participants ($n = 1060$, of whom 647 were female) were aged from 16 to 40 years [M = 22 years, standard deviation (SD) = 4 years]. They were recruited from the Cambridge area to participate in the PERGENIC project (Goodbourn *et al.* 2012; Lawrance-Owen *et al.* 2013). All participants reported European ancestry – as established by the nationality of their four grandparents – during initial screening. Subsequent checks on ancestry were made during genetic quality control procedures. Participants were paid £25 to complete a battery of tasks lasting about 2.5 h. After they had been given a full description of the study, and written informed consent was obtained. Participants were refracted to their best-corrected visual acuity [all ≤0.00 logMAR (logarithm of the minimum angle of resolution)]. To allow estimates of reliability, a randomly selected subsample ($n = 105$, of whom 66 were female) returned for a second identical session following a minimum interval of 1 week. The research was approved by the Psychology Research Ethics Committee of the University of Cambridge.

### Visual testing

The experiment was conducted in a darkened room. Stimuli were generated using MATLAB R2007b software, version 7.5 (The MathWorks Inc., Natick, MA, USA) with PsychToolbox-3 routines (Brainard 1997; Pelli 1997). They were processed on an nVidia EN9500GT video card (Asus, Taipei, Taiwan) driving a BITS++ video processor (Cambridge Research Systems, Rochester, UK) operating in MONO++ mode with a dynamic range of 14 bits. Stimuli were displayed on a gamma-corrected Trinitron GDM-F520 monitor (Sony Corporation, Tokyo, Japan) operating at a spatial resolution of 1024 × 768 pixels and a refresh rate of 100 Hz. Participants viewed stimuli monocularly using their dominant eye, or – if the difference in visual acuity between eyes was at least 0.10 logMAR – using the eye with better acuity; the other eye was occluded with a translucent patch. They used a headrest to maintain a viewing distance of 0.5 m, and gave responses using a two-button hand-held box.

The spatial profile of the stimulus is shown in Fig. 1a. It comprised a low spatial frequency sinusoidal luminance grating with a horizontal carrier ($f_S = 0.5$ c/deg, $\phi$ randomized on each trial) windowed by a two-dimensional Gaussian envelope with a SD of 2.0° (i.e. a vertically oriented Gabor), which reversed in contrast according to a 25-Hz square wave. It was displayed on a uniform background for 500 milliseconds, centered 9.0° to either the left or right of fixation, with contrast ramped on and off over 120 milliseconds according to a raised cosine envelope. The mean luminance of the display was 30 cd/m$^2$.

On each trial, the participant's task was to make a two-alternative forced-choice identification of the location of the stimulus (left or right). Auditory feedback was provided after each response. Participants completed an initial set of high-contrast practice trials to ensure that they understood the task. For experimental trials, luminance contrast was determined according to two independent randomly interleaved ZEST adaptive staircases (King-Smith *et al.* 1994; Watson & Pelli 1983), each comprising 30 trials. Michelson contrast at detection threshold was calculated as the 82% correct point of a cumulative Weibull psychometric function fitted to the pooled data from the two staircases. Sensitivity was defined as the inverse of threshold contrast.

### Genotyping

A 2-ml saliva sample was collected from each participant using an Oragene OG-500 kit (DNA Genotek Inc., Ottawa, ON, Canada). DNA was extracted and purified from 1064 samples by Cambridge Genomic Services (University of Cambridge, UK) according to the manufacturer's protocols. It was quantified using a PicoGreen fluorescence enhancement assay (Molecular Probes, Eugene, OR, USA), and its integrity was assessed by agarose gel electrophoresis. Samples were excluded if DNA concentration was below 30 ng/μl ($n = 34$) or if there was evidence of degradation ($n = 9$). Further samples ($n = 13$) were excluded at this stage owing to missing phenotypic data relating to other components of the PERGENIC project. The remaining 1008 samples were genotyped at 733 202 single nucleotide polymorphisms (SNPs) on the HumanOmniExpress BeadChip (Illumina, San Diego, CA, USA). Genotypes were called by custom clustering, using Illumina GenomeStudio software.

### Quality control

On the basis of genetic quality control, 20 samples were excluded from further analysis. Criteria for exclusion were as follows: sex anomaly, identified by examining X-chromosome heterozygosity and Y-chromosome missingness ($n = 3$); low individual genotyping call rate (<97% of SNPs called; $n = 1$); duplication of ($n = 4$) or relatedness to ($n = 11$) other samples, identified by examining estimates of identity-by-descent; and non-membership of a homogeneous population, identified by principal component analysis (PCA) using our PERGENIC genotypes, by combined PCA with HapMap3 genotypes (International Hapmap 3 Consortium 2010; International Hapmap Consortium 2005, 2007; Pemberton *et al.* 2010) and by hierarchical cluster analysis using pairwise identity-by-state as the distance metric ($n = 1$). The remaining samples belonged to 988 individuals. Three individuals, including one member of the retest subsample, lacked phenotypic data owing to equipment failure. This left 985 participants, 598 of whom were female, in the final genetic association analyses. Some individual SNP markers were also excluded from analysis on the basis of low coverage (called in <98% of individuals; $n = 12\,706$) or low minor allele frequency (<1%; $n = 77\,738$), leaving 642 758 SNPs in the final analyses.

### Statistical analysis

After assessing the power of the study across a large range of expected effect sizes (see Supporting Information Methods and Fig. S1), we performed genetic association analyses using PLINK v1.07 software (Purcell *et al.* 2007). Each SNP marker was tested for association with contrast sensitivity using linear regression under an allelic dosage model. Such a model assumes that the number of copies of the minor allele is related to the phenotypic measure in a linear fashion. For autosomal and pseudo-autosomal markers, major homozygotes were coded as 0, heterozygotes as 1 and minor homozygotes as 2. For other markers on the Y chromosome, individuals possessing the major allele were coded as 0 and individuals possessing the minor allele were coded as 1. For other markers on the X chromosome, females were coded as for an autosomal marker, and males as for a marker on the Y chromosome; sex was also included as a covariate in the analysis. We used the EIGENSTRAT method to control for any residual population stratification: the top three principal components of genetic variation in our sample were extracted with EIGENSOFT v4.2 software, and entered as covariates in the regression model (Patterson *et al.* 2006; Price *et al.* 2006; see Fig. S2). In addition, we used the permutation procedure implemented in PLINK to derive a familywise significance value for each association over 10 000 iterations ($P_{fw}$). In this case, we accounted for residual stratification by allowing the permutation of phenotypes only within population groups defined in our hierarchical cluster analysis.

For each marker suggestive of association ($P_{unadjusted} < 10^{-5}$), we evaluated the distribution of genotypes for deviation from Hardy–Weinberg equilibrium and manually inspected the signal intensity cluster plot. We then defined 2.5-Mbp regions of interest surrounding all suggestive loci, and imputed genotypes within these regions with IMPUTE v2.3.0 software (Howie *et al.* 2009, 2011) using the phased haplotypes of the 1000 Genomes Project as a reference panel (Abecasis *et al.* 2010). Rather than preselect specific European populations within the panel, we allowed the imputation algorithm to select a custom reference panel for each haplotype based on local sequence similarity (Howie *et al.* 2009). We completed association analysis for the imputed SNP genotype probabilities using the dosage association feature of PLINK, with the three principal component axes entered as covariates. Genotype data were converted between PLINK and IMPUTE formats using GTOOL v0.7.5 software. Genomic references were based on the Human February 2009 (GRCh37/hg19) assembly sequence.

## Results

Contrast sensitivity, defined as the inverse of Michelson contrast at threshold, ranged from 2.5 to 74.7, with a median of 33.8. The distribution was approximately normal, with a mean of 34.1 and SD of 10.2 (Fig. 1b). We observed no significant difference in mean sensitivity between males ($M = 34.7$, $SD = 9.9$) and females ($M = 33.8$, $SD = 10.3$); $t(1052) = 1.52$, $P = 0.13$. Test–retest reliability was high, as indicated by the correlation between sensitivity measured in the first and second sessions for the subsample of participants who completed the task twice (Pearson's $r = 0.71$, $P \ll 0.001$; Fig. 1c). The 95% limits of agreement on the measurement were $0.2 \pm 17.2$ (Fig. 1d).

The quantile–quantile plot for the results of the genome-wide association analysis (Fig. 2a) provides evidence of significant deviation from the null hypothesis of no association of the phenotype with any SNP genome-wide, for $P$ values below about $10^{-5}$. The shape of the plot, together with the value of the genomic inflation factor ($\lambda = 1.00$) (Devlin & Roeder 1999), suggests that test statistics were not inflated by technical error or by population stratification. The genome-wide Manhattan plot (Fig. 2b) reveals several

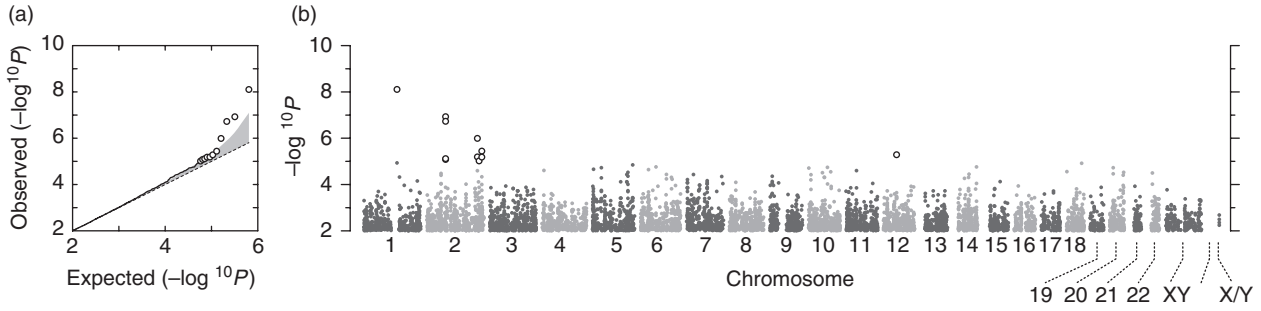


**Figure 2: Genome-wide association analyses**. (a) Genome-wide quantile–quantile plot. For each SNP, the negative logarithm of the linear association test $P$ value (solid line, $P < 10^{-5}$; open circles $P > 10^{-5}$) is plotted against the expected value for the quantile corresponding to that SNP under the null hypothesis of no genome-wide association. The diagonal dashed line shows the relationship expected under the null hypothesis, and the shaded region shows the 95% confidence interval. (b) Genome-wide Manhattan plot. For each SNP, the negative logarithm of the linear association test $P$ value (solid circles, $P < 10^{-5}$; open circles $P > 10^{-5}$) is plotted against position on the chromosome.

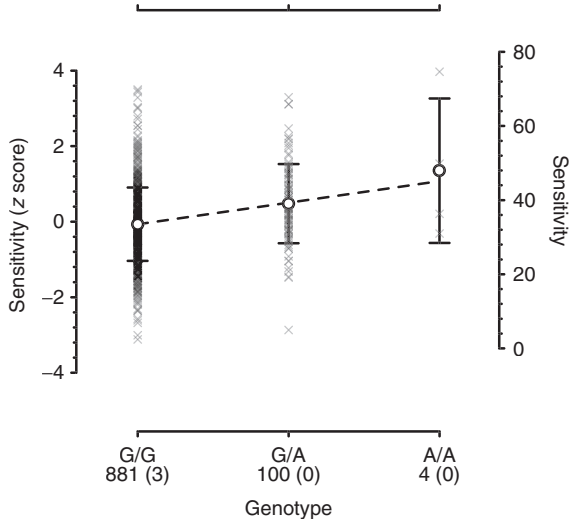


**Figure 3: Contrast sensitivity as a function of genotype at SNP marker rs1797052**. Individual sensitivities are shown as crosses, and genotype means are shown as open icons, with error bars representing ±1 SD. The dashed line is derived by linear regression of sensitivity on genotype. Genotype labels refer to individuals homozygous for the major allele (G/G), heterozygous individuals (G/A) and individuals homozygous for the minor allele (A/A). Below each genotype label is the number of individuals called with that genotype who have non-missing and missing phenotypic data, respectively.

regions suggestive of association with contrast sensitivity, situated on chromosomes 1, 2 and 12. Here, we consider the region containing the strongest evidence of association (other genomic regions are detailed in Supporting Information Results and Discussion, Tables S1,S2 and Figs. S3,S4).

The strongest association signal was at the SNP marker rs1797052, situated on chromosome 1q21.1 ($P = 7.9 \times 10^{-9}$; $P_{fw} = 0.005$). Each additional copy of the minor allele (frequency 5.5%) was linked to an increase in contrast sensitivity equivalent to 0.56 SDs (Fig. 3). There was no evidence of departure from Hardy–Weinberg equilibrium ($P = 0.53$), and inspection of the signal intensity cluster plot shows that genotype calling was successful (see Fig. S5). The marker rs1797052 is situated in the 5′-untranslated region of the gene *PDZK1*; the surrounding 2.5-Mbp region of interest is shown in Fig. 4a.

The genotyped marker with the next strongest association (rs1284300, $P = 1.2 \times 10^{-5}$) is intronic to *PDZK1*, positioned 211 bp downstream of the first coding region. This marker is in relatively high linkage disequilibrium with rs1797052 ($r^2 = 0.44$, $D' = 0.78$), and the association is eliminated if the analysis is conditioned on rs1797052 ($P = 0.43$). Genotype imputation in this region revealed evidence of another SNP associated with contrast sensitivity, rs17352344 ($P = 5.6 \times 10^{-6}$); it is situated in the 3′-untranslated region of *PIAS3*, upstream of *PDZK1*. This marker is also in relatively high linkage disequilibrium with rs1797052 ($r^2 = 0.29$, $D' = 0.74$), and the association is eliminated if the analysis is conditioned on rs1797052 ($P = 0.75$).

## Discussion

*PDZK1* encodes the protein PDZK1 (PDZ domain containing 1), one member of a family of PDZ domain-containing scaffold proteins that hold other proteins in the appropriate configuration. PDZ domains are phylogenetically ancient sequences of amino acids that bind to other proteins. PDZK1 has four such domains, and specifically mediates the localization of cell surface proteins (Fanning & Anderson 1999).

The complex comprising PDZK1, DLG4, SYNGAP1, KLHL17 and *N*-methyl-D-aspartate (NMDA) receptors is crucial in maintaining the integrity of the actin cytoskeleton in neurons (Chen & Li 2005). Actin microfilaments provide cellular structure, and allow cell motility by providing tracks for myosin molecules. That PDZK1 interacts with NMDA receptors is notable in the current context because the latter play a critical role in regulating contrast gain control mechanisms in the retinogeniculate system (Kwon *et al.* 1992). Indeed, it has already been hypothesized that the perceptual abnormalities observed in schizophrenia – including deficits in contrast sensitivity – might arise from a dysfunction of NMDA receptors (Javitt 2003).

The neuroligin NLGN1 binds to at least one component (DLG4) of the PDZK1 complex (Meyer *et al.* 2004) through a PDZ domain-binding site in its cytoplasmic tail (Craig & Kang 2007). Neuroligins are postsynaptic membrane proteins that mediate synaptic formations, a process believed to be regulated by DLG4 (Huang *et al.* 2000). Neuroligin genes have been implicated previously in ASD susceptibility (Bourgeron 2009; Sudhof 2008), and disruption of murine *Dlg4* produces a phenotype with several of the behavioral and neurological features of ASD (Feyder *et al.* 2010).

The strongest association was observed at a marker in the 5′-untranslated region of *PDZK1*, indicating that the critical genetic variant may be situated within a regulatory element. We note that the secondary association within the 1q21.1 region is with an imputed marker (rs17352344) in the gene *PIAS3*, which encodes a transcriptional modulator that binds to transcription factors. At least one of its partners, TATA-binding protein (TBP), has a binding site that includes the primary association marker rs1797052, immediately upstream of *PDZK1* (Fig. 4b) (Prigge & Schmidt 2006).

*PDZK1* falls within a well-established schizophrenia susceptibility locus on chromosome 1q21.1. Early studies conducted within several different populations revealed linkage in large expanses (up to nearly 30 Mbp) of the wider 1q21–1q23 region (Brzustowicz *et al.* 2000; Gurling *et al.* 2001; Hwu *et al.* 2003; Shaw *et al.* 1998; Zheng *et al.* 2006). Recently, *de novo* deletion (International Schizophrenia Consortium 2008; Levinson *et al.* 2011; Stefansson *et al.* 2008) and duplication (Levinson *et al.* 2012) in a ∼1.5 Mbp region encompassing *PDZK1* have been implicated in schizophrenia in independent case–control and family studies. One candidate gene study has also reported an association between schizophrenia and two SNPs in the region (Ni *et al.* 2007).

The same locus is also a recognized risk region for ASD. Initial comparative hybridization studies pointed to a rare recurrent duplication situated on 1q21.1, downstream of *PDZK1* (Mefford *et al.* 2008; Szatmari *et al.* 2007).

Subsequent studies, however, have identified rare deletions (Pinto *et al.* 2010) and duplications (Pinto *et al.* 2010; Sanders *et al.* 2011) directly involving the gene. Furthermore, using a novel homozygous haplotype mapping approach, Casey *et al.* (2012) identified ASD-specific risk haplotypes at 1q21.1 in three different population clusters; only *PDZK1* was situated in the genetic region shared by all three haplotypes.

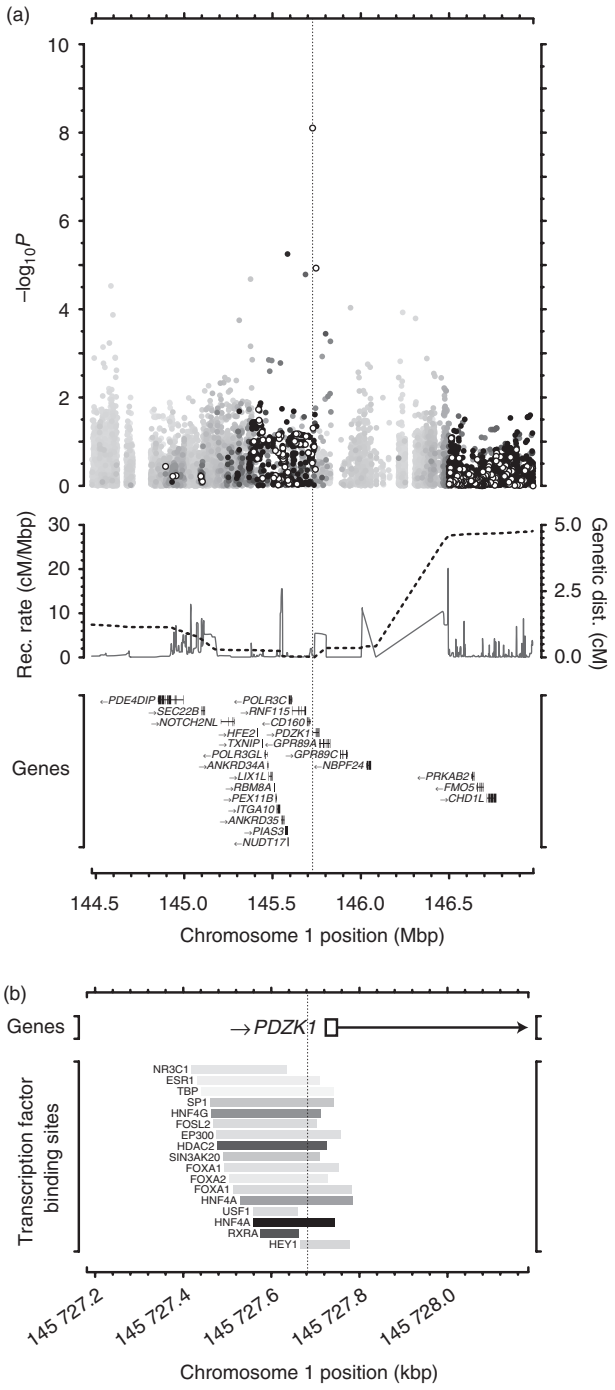


The association between variants in a genetic risk region for schizophrenia and ASD and sensitivity to frequency-doubled gratings is particularly notable because abnormalities in sensitivity constitute a promising endophenotype for both disorders. Gottesman and Gould (2003) propose five criteria useful for identifying endophenotypes of psychological disorder. First, the endophenotype should be associated with the disorder: The studies previously reviewed indicate that abnormal sensitivity to frequency-doubled stimuli is associated with both schizophrenia and autism. Second, the endophenotype should be heritable: contrast sensitivity to targets of low spatial frequency and high temporal frequency has been shown to be highly heritable ($H^2 = 0.70$) in a classical twin study (Hogg *et al.* 2009). Third, the endophenotype should be primarily state-independent. In schizophrenia, abnormal sensitivities are evident in prodromal (Kéri & Benedek 2007), first-episode unmedicated (Kiss *et al.* 2010), chronic unmedicated (Kéri *et al.* 2004, 2005b) and chronic medicated states (Butler *et al.* 2005; Gracitelli *et al.* 2013; Kéri *et al.* 2005a). Autism spectrum disorder is not episodic in the same manner as schizophrenia, so it is not clear how state independence might be demonstrated. The fourth criterion is that the endophenotype and illness should co-segregate within families, but we are unaware of any study to date that has investigated co-segregation of schizophrenia with abnormal contrast sensitivity. Finally, the endophenotype should be found in unaffected family members at a higher rate than in the general population. In schizophrenia, abnormal contrast sensitivity is found in unaffected siblings (Kéri *et al.* 2004, 2005a) and in unaffected parents (Gracitelli *et al.* 2013). In ASD, abnormal sensitivity has been found in unaffected 'high-risk' infants with an older affected sibling – at most, only 1 of the 18 high-risk infants was expected to develop

**Figure 4: Association region on chromosome 1q21.1**. (a) Manhattan plot of 2.5-Mbp region centered on rs1797052. Top: negative logarithm of the linear association *P* value for each SNP, plotted against position of the SNP on the chromosome. Genotyped SNPs are shown as open icons; imputed SNPs are shown on a scale from white to black, with darkness proportional to confidence in the imputation. Several expanses in the region have a low density of genotyped SNP markers on the HumanOmniExpress BeadChip, which leads to low confidence in imputed SNP markers. Critically, however, the expanse containing *PDZK1* has appropriate SNP density and high imputation quality. Middle: fine-scale recombination rate (Rec. rate, light solid line) and cumulative genetic distance from rs1797052 (Genetic dist., dark dashed line) estimated from 1000 Genomes Phase I data (Abecasis *et al.* 2010). Bottom: genes in the region, with exons represented as vertical rectangles. The gene symbol is shown to the right of each gene, and the arrow indicates the direction of transcription. (b) Transcription factor binding sites upstream of *PDZK1* as assayed by chromatin immunoprecipitation sequencing (ChIP-seq). Each rectangle represents the region encompassing peaks of transcription factor occupancy, with darkness proportional to signal strength. Data are derived from the ENCODE Transcription Factor ChIP-seq track of the UCSC Genome Browser (Rosenbloom *et al.* 2013). In both panels, the vertical dotted line denotes the position of rs1797052.

ASD (McCleery *et al.* 2007). In summary, by these criteria, contrast sensitivity to stimuli of low spatial frequency and high temporal frequency is a promising endophenotype of schizophrenia and ASD.

Our results suggest that variation in *PDZK1*, situated in the 1q21.1 susceptibility region for schizophrenia and ASD, affects visual sensitivity to stimuli of low spatial frequency and high temporal frequency in a psychologically normal population. While this study had appropriate power to detect effects of the size observed for the marker rs1797052 (see Supporting Information), it is nonetheless likely that our estimate of effect size is inflated to some extent by the so-called *winner's curse* (Lohmueller *et al.* 2003), and this should be considered in the design of confirmatory studies. Replication in an independent panel will be a critical next step in using our findings to inform future functional investigations. Such functional research should focus on identifying and clarifying the biological mechanisms, such as neuroligin and NMDA receptor function, through which *PDZK1* might exert its pleiotropic effects.

## References


Abecasis, G.R., Altshuler, D., Auton, A., Brooks, L.D., Durbin, R.M., Gibbs, R.A., Hurles, M.E. & McVean, G.A. (2010) A map of human genome variation from population-scale sequencing. *Nature* **467**, 1061–1073.

Bourgeron, T. (2009) A synaptic trek to autism. *Curr Opin Neurobiol* **19**, 231–234.

Braff, D.L. & Freedman, R. (2002) Endophenotypes in studies of the genetics of schizophrenia. In Davis, K.L., Charney, D., Coyle, J.T. & Nemeroff, C. (eds), *Neuropsychopharmacology: The Fifth Generation of Progress*. Lippincott Williams & Wilkins, Philadelphia, PA, pp. 703–716.

Brainard, D.H. (1997) The psychophysics toolbox. *Spat Vis* **10**, 433–436.

Brzustowicz, L.M., Hodgkinson, K.A., Chow, E.W., Honer, W.G. & Bassett, A.S. (2000) Location of a major susceptibility locus for familial schizophrenia on chromosome 1q21-q22. *Science* **288**, 678–682.

Butler, P.D., Zemon, V., Schechter, I., Saperstein, A.M., Hoptman, M.J., Lim, K.O., Revheim, N., Silipo, G. & Javitt, D.C. (2005) Early-stage visual processing and cortical amplification deficits in schizophrenia. *Arch Gen Psychiatry* **62**, 495–504.

Butler, P.D., Silverstein, S.M. & Dakin, S.C. (2008) Visual perception and its impairment in schizophrenia. *Biol Psychiatry* **64**, 40–47.

Casey, J.P., Magalhaes, T., Conroy, J.M. *et al.* (2012) A novel approach of homozygous haplotype sharing identifies candidate genes in autism spectrum disorder. *Hum Genet* **131**, 565–579.

Chen, Y. & Li, M. (2005) Interactions between CAP70 and actinfilin are important for integrity of actin cytoskeleton structures in neurons. *Neuropharmacology* **49**, 1026–1041.

Craig, A.M. & Kang, Y. (2007) Neurexin-neuroligin signaling in synapse development. *Curr Opin Neurobiol* **17**, 43–52.

Dakin, S. & Frith, U. (2005) Vagaries of visual perception in autism. *Neuron* **48**, 497–507.

Devlin, B. & Roeder, K. (1999) Genomic control for association studies. *Biometrics* **55**, 997–1004.

Fanning, A.S. & Anderson, J.M. (1999) PDZ domains: fundamental building blocks in the organization of protein complexes at the plasma membrane. *J Clin Invest* **103**, 767–772.

Feyder, M., Karlsson, R.M., Mathur, P. *et al.* (2010) Association of mouse Dlg4 (PSD-95) gene deletion and human DLG4 gene variation with phenotypes relevant to autism spectrum disorders and Williams' syndrome. *Am J Psychiatry* **167**, 1508–1517.

Goodbourn, P.T., Bosten, J.M., Hogg, R.E., Bargary, G., Lawrance-Owen, A.J. & Mollon, J.D. (2012) Do different 'magnocellular tasks' probe the same neural substrate? *Proc Biol Sci* **279**, 4263–4271.

Gottesman, I.I. & Gould, T.D. (2003) The endophenotype concept in psychiatry: etymology and strategic intentions. *Am J Psychiatry* **160**, 636–645.

Gracitelli, C.P.B., Vaz de Lima, F.B., Bressan, R.A. & Paranhos, A. Jr. (2013) Visual field loss in schizophrenia: evaluation of magnocellular pathway dysfunction in schizophrenic patients and their parents. *Clin Ophthalmol* **7**, 1015–1021.

Greenaway, R., Davis, G. & Plaisted-Grant, K. (2013) Marked selective impairment in autism on an index of magnocellular function. *Neuropsychologia* **51**, 592–600.

Greenwood, T.A., Lazzeroni, L.C., Murray, S.S. *et al.* (2011) Analysis of 94 candidate genes and 12 endophenotypes for schizophrenia from the Consortium on the Genetics of Schizophrenia. *Am J Psychiatry* **168**, 930–946.

Greenwood, T.A., Light, G.A., Swerdlow, N.R., Radant, A.D. & Braff, D.L. (2012) Association analysis of 94 candidate genes and schizophrenia-related endophenotypes. *PLoS One* **7**, e29630.

Greenwood, T.A., Swerdlow, N.R., Gur, R.E. *et al.* (2013) Genome-wide linkage analyses of 12 endophenotypes for schizophrenia from the Consortium on the Genetics of Schizophrenia. *Am J Psychiatry* **170**, 521–532.

Grinter, E.J., Maybery, M.T. & Badcock, D.R. (2010) Vision in developmental disorders: is there a dorsal stream deficit? *Brain Res Bull* **82**, 147–160.

Gurling, H.M., Kalsi, G., Brynjolfson, J., Sigmundsson, T., Sherrington, R., Mankoo, B.S., Read, T., Murphy, P., Blaveri, E., McQuillin, A., Petursson, H. & Curtis, D. (2001) Genomewide genetic linkage analysis confirms the presence of susceptibility loci for schizophrenia, on chromosomes 1q32.2, 5q33.2, and 8p21-22 and provides support for linkage to schizophrenia, on chromosomes 11q23.3-24 and 20q12.1-11.23. *Am J Hum Genet* **68**, 661–673.

Hogg, R.E., Dimitrov, P.N., Dirani, M., Varsamidis, M., Chamberlain, M.D., Baird, P.N., Guymer, R.N. & Vingrys, A.J. (2009) Gene–environment interactions and aging visual function: a classical twin study. *Ophthalmology* **116**, 263–269.

Howie, B.N., Donnelly, P. & Marchini, J. (2009) A flexible and accurate genotype imputation method for the next generation of genome-wide association studies. *PLoS Genet* **5**, e1000529.

Howie, B., Marchini, J. & Stephens, M. (2011) Genotype imputation with thousands of genomes. *G3 (Bethesda)* **1**, 457–470.

Huang, Y.Z., Won, S., Ali, D.W., Wang, Q., Tanowitz, M., Du, Q.S., Pelkey, K.A., Yang, D.J., Xiong, W.C., Salter, M.W. & Mei, L. (2000) Regulation of neuregulin signaling by PSD-95 interacting with ErbB4 at CNS synapses. *Neuron* **26**, 443–455.

Hwu, H.G., Liu, C.M., Fann, C.S., Ou-Yang, W.C. & Lee, S.F. (2003) Linkage of schizophrenia with chromosome 1q loci in Taiwanese families. *Mol Psychiatry* **8**, 445–452.

International HapMap 3 Consortium (2010) Integrating common and rare genetic variation in diverse human populations. *Nature* **467**, 52–58.

International HapMap Consortium (2005) A haplotype map of the human genome. *Nature* **437**, 1299–1320.

International HapMap Consortium (2007) A second generation human haplotype map of over 3.1 million SNPs. *Nature* **449**, 851–861.

International Schizophrenia Consortium (2008) Rare chromosomal deletions and duplications increase risk of schizophrenia. *Nature* **455**, 237–241.

Javitt, D.C. (2003) Peeling the onion: NMDA dysfunction as a unifying model in schizophrenia. *Behav Brain Sci* **26**, 93–94.

Kéri, S. & Benedek, G. (2007) Visual contrast sensitivity alterations in inferred magnocellular pathways and anomalous perceptual experiences in people at high-risk for psychosis. *Vis Neurosci* **24**, 183–189.

Kéri, S., Kelemen, O., Benedek, G. & Janka, Z. (2004) Vernier threshold in patients with schizophrenia and in their unaffected siblings. *Neuropsychology* **18**, 537–542.

Kéri, S., Kelemen, O., Janka, Z. & Benedek, G. (2005a) Visual-perceptual dysfunctions are possible endophenotypes of schizophrenia: evidence from the psychophysical investigation of magnocellular and parvocellular pathways. *Neuropsychology* **19**, 649–656.

Kéri, S., Kiss, I., Kelemen, O., Benedek, G. & Janka, Z. (2005b) Anomalous visual experiences, negative symptoms, perceptual organization and the magnocellular pathway in schizophrenia: a shared construct? *Psychol Med* **35**, 1445–1455.

King-Smith, P.E., Grigsby, S.S., Vingrys, A.J., Benes, S.C. & Supowit, A. (1994) Efficient and unbiased modifications of the QUEST threshold method: theory, simulations, experimental evaluation and practical implementation. *Vision Res* **34**, 885–912.

Kiss, I., Fábián, A., Benedek, G. & Kéri, S. (2010) When doors of perception open: visual contrast sensitivity in never-medicated, first-episode schizophrenia. *J Abnorm Psychol* **119**, 586–593.

Kwon, Y.H., Nelson, S.B., Toth, L.J. & Sur, M. (1992) Effect of stimulus contrast and size on NMDA receptor activity in cat lateral geniculate nucleus. *J Neurophysiol* **68**, 182–196.

Lawrance-Owen, A.J., Bargary, G., Bosten, J.M., Goodbourn, P.T., Hogg, R.E. & Mollon, J.D. (2013) Genetic association suggests that SMOC1 mediates between prenatal sex hormones and digit ratio. *Hum Genet* **132**, 415–421.

Levinson, D.F., Duan, J., Oh, S. *et al.* (2011) Copy number variants in schizophrenia: confirmation of five previous findings and new evidence for 3q29 microdeletions and VIPR2 duplications. *Am J Psychiatry* **168**, 302–316.

Levinson, D.F., Shi, J., Wang, K. *et al.* (2012) Genome-wide association study of multiplex schizophrenia pedigrees. *Am J Psychiatry* **169**, 963–973.

Lohmueller, K.E., Pearce, C.L., Pike, M., Lander, E.S. & Hirschhorn, J.N. (2003) Meta-analysis of genetic association studies supports a contribution of common variants to susceptibility to common disease. *Nat Genet* **33**, 177–182.

Maddess, T. (2011) Frequency-doubling technology and parasol cells. *Invest Ophthalmol Vis Sci* **52**, 3759.

McCleery, J.P., Allman, E., Carver, L.J. & Dobkins, K.R. (2007) Abnormal magnocellular pathway visual processing in infants at risk for autism. *Biol Psychiatry* **62**, 1007–1014.

Mefford, H.C., Sharp, A.J., Baker, C. *et al.* (2008) Recurrent rearrangements of chromosome 1q21.1 and variable pediatric phenotypes. *N Engl J Med* **359**, 1685–1699.

Meyer, G., Varoqueaux, F., Neeb, A., Oschlies, M. & Brose, N. (2004) The complexity of PDZ domain-mediated interactions at glutamatergic synapses: a case study on neuroligin. *Neuropharmacology* **47**, 724–733.

Ni, X., Valente, J., Azevedo, M.H., Pato, M.T., Pato, C.N. & Kennedy, J.L. (2007) Connexin 50 gene on human chromosome 1q21 is associated with schizophrenia in matched case control and family-based studies. *J Med Genet* **44**, 532–536.

Patterson, N., Price, A.L. & Reich, D. (2006) Population structure and eigenanalysis. *PLoS Genet* **2**, e190.

Pelli, D.G. (1997) The VideoToolbox software for visual psychophysics: transforming numbers into movies. *Spat Vis* **10**, 437–442.

Pemberton, T.J., Wang, C., Li, J.Z. & Rosenberg, N.A. (2010) Inference of unexpected genetic relatedness among individuals in HapMap Phase III. *Am J Hum Genet* **87**, 457–464.

Pinto, D., Pagnamenta, A.T., Klei, L. *et al.* (2010) Functional impact of global rare copy number variation in autism spectrum disorders. *Nature* **466**, 368–372.

Price, A.L., Patterson, N.J., Plenge, R.M., Weinblatt, M.E., Shadick, N.A. & Reich, D. (2006) Principal components analysis corrects for stratification in genome-wide association studies. *Nat Genet* **38**, 904–909.

Prigge, J.R. & Schmidt, E.E. (2006) Interaction of protein inhibitor of activated STAT (PIAS) proteins with the TATA-binding protein, TBP. *J Biol Chem* **281**, 12260–12269.

Purcell, S., Neale, B., Todd-Brown, K., Thomas, L., Ferreira, M.A., Bender, D., Maller, J., Sklar, P., de Bakker, P.I., Daly, M.J. & Sham, P.C. (2007) PLINK: a tool set for whole-genome association and population-based linkage analyses. *Am J Hum Genet* **81**, 559–575.

Rosenbloom, K.R., Sloan, C.A., Malladi, V.S. *et al.* (2013) ENCODE data in the UCSC Genome Browser: year 5 update. *Nucleic Acids Res* **41**, D56–D63.

Rosli, Y., Bedford, S. & Maddess, T. (2009) Low spatial-frequency channels and the spatial frequency doubling illusion. *Invest Ophthalmol Vis Sci* **50**, 1956–1963.

Sanders, S.J., Ercan-Sencicek, A.G., Hus, V. *et al.* (2011) Multiple recurrent de novo CNVs, including duplications of the 7q11.23 Williams syndrome region, are strongly associated with autism. *Neuron* **70**, 863–885.

Shaw, S.H., Kelly, M., Smith, A.B., Shields, G., Hopkins, P.J., Loftus, J., Laval, S.H., Vita, A., De Hert, M., Cardon, L.R., Crow, T.J., Sherrington, R. & DeLisi, L.E. (1998) A genome-wide search for schizophrenia susceptibility genes. *Am J Med Genet* **81**, 364–376.

Simmons, D.R., Robertson, A.E., McKay, L.S., Toal, E., McAleer, P. & Pollick, F.E. (2009) Vision in autism spectrum disorders. *Vision Res* **49**, 2705–2739.

Stefansson, H., Rujescu, D., Cichon, S. *et al.* (2008) Large recurrent microdeletions associated with schizophrenia. *Nature* **455**, 232–236.

Sudhof, T.C. (2008) Neuroligins and neurexins link synaptic function to cognitive disease. *Nature* **455**, 903–911.

Szatmari, P., Paterson, A.D., Zwaigenbaum, L. *et al.* (2007) Mapping autism risk loci using genetic linkage and chromosomal rearrangements. *Nat Genet* **39**, 319–328.

Watson, A.B. & Pelli, D.G. (1983) QUEST: a Bayesian adaptive psychometric method. *Percept Psychophys* **33**, 113–120.

Zheng, Y., Wang, X., Gu, N., Feng, G., Zou, F., Qin, W., Zhang, J., Lin, W., Tao, R., Qian, X. & He, L. (2006) A two-stage linkage analysis of Chinese schizophrenia pedigrees in 10 target chromosomes. *Biochem Biophys Res Commun* **342**, 1049–1057.

## Acknowledgments

This work was supported by the Gatsby Charitable Foundation (GAT2903). P.T.G. was supported by a scholarship from the Cambridge Commonwealth and Overseas Trusts, and by an Overseas Research Studentship from the U.K. Government. The authors are grateful to Horace Barlow, Roger Freedman, Graeme Mitchison and Richard Durbin for their role in the initiation of the PERGENIC project, and to Julien Bauer, Emily Clemente and Kerry Cliffe of Cambridge Genomic Services for their valuable help. The authors declare no conflict of interest.

## Supporting Information

Additional supporting information may be found in the online version of this article at the publisher's web-site:

**Appendix S1**. Details of five genomic regions suggestive of association with frequency-doubled grating sensitivity.

**Table S1:** Genotyped SNPs showing evidence of association with frequency-doubled grating sensitivity.

**Table S2:** Imputed SNPs showing evidence of association with frequency-doubled grating sensitivity.

**Figure S1:** Power analysis of this study. (a) Power to detect a nominally significant association ($P < 5 \times 10^{-7}$). Effect size is the coefficient of determination ($R^2$) between the causal variant and the phenotype. The red line illustrates the case in which the causal variant is in perfect linkage disequilibrium ($r^2 = 1.00$) with a genotyped SNP; the dashed lines illustrate cases where the causal variant is in imperfect linkage

disequilibrium with a genotyped SNP, $r^2 = 0.95–0.05$ (in steps of 0.05). (b) Power to detect a suggestive association ($P < 10^{-5}$). (c) Histograms showing the expected proportion of known SNPs for which the maximum $r^2$ with a genotyped SNP falls in 1 of 11 bins; the red bar shows the expected proportion of known SNPs in perfect linkage disequilibrium with a genotyped SNP. Data are from Spencer *et al.* (2009) for the Illumina 610K assay, which has slightly lower coverage than the assay used in this study.

**Figure S2:** Principal components entered as covariates in the analysis to correct for residual population stratification. (a) Three-dimensional scatter plot of participants on the first three principal component (PC) axes. Individuals are color-coded according to the population cluster assigned during hierarchical cluster analysis using pairwise identity-by-state (IBS) as the distance metric. These clusters were used to control for population stratification in the permutation procedure. (b) Histograms of individual PC score on the first three PC axes. Six individuals had PC scores between 0.2 and 0.5 on the third PC.

**Figure S3:** Manhattan plots of 2.5-Mbp supplementary genomic regions suggestive of association with frequency-doubled grating sensitivity. Top: negative logarithm of the linear association test *P* value for each SNP plotted against position on the chromosome. Genotyped SNPs are shown as red icons; imputed SNPs are shown on a scale from white to black, with darkness proportional to confidence in the imputation. Middle: fine-scale recombination rate (dark solid line) and cumulative genetic distance from index SNP marker (red dashed line) estimated from 1000 Genomes Phase I data (Abecasis *et al.* 2010). Bottom: genes in the region, with exons shown as vertical rectangles. In all panels, vertical dotted lines mark the boundaries of the subregion of interest. (a) Chromosome 2p12 association region centered on SNP marker rs11683503. (b) Chromosome 2q34 association region centered on SNP marker rs1510552. (c) Chromosome 2q36.1 association region centered on SNP marker rs10498101. (d) Chromosome 2q37.1 association region centered on SNP marker rs2233375. (e) Chromosome 12q13.2 association region centered on SNP marker rs12230513.

**Figure S4:** Contrast sensitivity as a function of genotype at index SNP markers for each supplementary genomic region suggestive of association with frequency-doubled grating sensitivity. Individual sensitivities are shown as crosses, and genotype means are shown as open icons, with error bars representing ±1 standard deviation. The dashed line is derived by linear regression of sensitivity on genotype. Genotype labels below the axes refer to individuals homozygous for the major allele, heterozygous individuals, individuals homozygous for the minor allele and individuals with missing genetic data, respectively. Below each genotype label is the number of individuals called with that genotype who have non-missing and missing phenotypic data, respectively. (a) SNP marker rs11683503 on chromosome 2p12. (b) SNP marker rs1510552 on chromosome 2q34. (c) SNP marker rs10498101 on chromosome 2q36.1. (d) SNP marker rs2233375 on chromosome 2q37.1. (e) SNP marker rs12230513 on chromosome 12q13.2.

**Figure S5:** Signal intensity cluster plots for SNPs suggestive of association with frequency-doubled grating sensitivity. All genotyped participants are shown; individuals included in the analysis are represented by circles, and individuals excluded on the basis of genetic quality control are represented by crosses. Major homozygotes are shown in blue, heterozygotes in purple, minor homozygotes in red and unsuccessfully called genotypes in black. Shaded regions are the minimum ellipses that bound all individuals called for a genotype.